RSC Advances

PAPER

View Article Online
View Journal | View Issue

Cite this: *RSC Adv.*, 2017, **7**, 45022

Facile, simple, and inexpensive ionic liquid, 1-phenyl-3-methylimidazole diphenyl phosphate, as an efficient phosphorus-based ligand for copper-catalyzed reverse atom transfer radical polymerization of methyl methacrylate

Xiao-hui Liu, * Qian Zhu, Yan-guang Zhang, Qiu-yan Zhang, Chen Ding and Jun Li

Ligands play a vital role in atom transfer radical polymerization (ATRP) in solubilizing the transition-metal salt and adjusting the redox potential of the metal center. In general, nitrogen ligands work particularly well for copper-mediated ATRP, while phosphorus-based ligands are rarely used due to less effectiveness. Therefore, this work aims to explore for the first time a facile, simple, and inexpensive ionic liquid (IL), 1-phenyl-3-methylimidazole diphenyl phosphate ([Phmim][Ph_2PO_4]), as an efficient phosphorus ligand for $CuBr_2$-mediated reverse ATRP. The key to success is ascribed to stronger complexation of the IL ligand with the catalyst and higher solubility of the resulting complex. The polymerizations proceeded in a controlled/"living" fashion, as evidenced by first-order kinetics, linear evolution of molecular weights with monomer conversion, and narrow molecular weight distributions. Effects of various experimental parameters—solvent, reaction temperature, IL, and molar ratio of $CuBr_2$/[Phmim][Ph_2PO_4]—on the polymerization were investigated in detail. Furthermore, ^{1}H NMR analysis confirmed the halogen-containing chain-end functionality of the resultant polymer.

Received 18th August 2017
Accepted 14th September 2017

DOI: 10.1039/c7ra09154k

rsc.li/rsc-advances

Introduction

Atom transfer radical polymerization (ATRP) has attracted considerable interest over the past twenty years because it can easily synthesize vinyl polymers with well-controlled molecular weights, narrow molecular weight distributions, and functional end-functionalities.[1–5] Normal ATRP proceeds *via* a redox process where an alkyl halide is activated by a transition-metal catalyst, generating the corresponding alkyl radical and the transition-metal complex in its higher oxidation state.[6–9] One serious disadvantage of ATRP is the air sensitivity of transition-metal complexes in their lower oxidation states.[10] Reverse ATRP was developed to overcome the above drawback. It has two advantages in comparison with normal ATRP: a conventional radical initiator is used instead of an organic halide, which is generally toxic and expensive, and the transition-metal complex in its higher oxidation state is air-stable.[11]

Generally, ligand plays key role in solubilizing the transition-metal complex and in adjusting the redox potential of the metal center for appropriate reactivity in a ATRP process.[12] Generally, nitrogen ligands work particularly well for copper-mediated ATRP but phosphorus-based ligands are rarely used ATRP due to less effectiveness. Ionic liquids (ILs) have drawn significant attention in the past few years. They have unique properties, such as low vapor pressure, non-flammability, and good solubility to transition-metal catalyst. Particularly, they are used as alternative for reaction media, extraction solvent for separation and recovery, and particularly used as ligand for ATRP.[13–16]

To date, there have many studies on ILs as reaction media or ligand for ATRP.[17–26] The use of 1-butyl-3-methylimidazolium hexafluorophosphate ([C_4mim][PF_6]) as solvent for copper(I)-mediated ATRP of methyl methacrylate (MMA) was first reported by Carmichael *et al.*[27] This report opened an avenue to the preparation of well-defined polymers by ATRP with IL as ligand. Particularly, IL as ligand instead of expensive nitrogen compounds for copper-catalyzed ATRP systems is possible. Matyjaszewski's group investigated copper(I) and iron(II)-catalyzed normal ATRP of MMA with various ILs as ligands.[28] These ILs with 1-alkyl-3-methylimidazolium ([Rmim], R represents an alkyl group) as cations contained different anions such as Cl^-, Br^-, CO_3^-, $AlCl_4^-$, $[(C_4H_9)_2PO_4]^-$, and *etc.* Furthermore, Lai's group explored the [Hmim][RCOO] used as ligand, ethyl 2-bromoisobutyrate/CuBr as the initiating system for normal ATRP of MMA.[29,30] However, all of above mentioned copper-IL catalyzed systems were used for normal ATRP. To the best of our knowledge, only Zhou's group[31,32] and Chen's group[33] had used IL as solvent for copper(II)-catalyzed reverse ATRP. The ILs in these polymerization systems generally used expensive

School of Materials Science and Engineering, State Key Laboratory of Separation Membranes and Membrane Processes, Tianjin Polytechnic University, Tianjin 300387, China. E-mail: liuxiaohui@tjpu.edu.cn

anion, such as PF_6^-, BF_4^-, and an organic ligand was usually required. Thus, it is curious to us why copper(II)-catalyzed reverse ATRP with IL as ligand was rarely reported.

The aim of this work is to prove the feasibility of the application of a novel IL, 1-phenyl-3-methylimidazole diphenyl phosphate ([Phmim][Ph_2PO_4]) as efficient phosphorus ligand for copper(II)-catalyzed reverse ATRP of MMA. Controlled/living polymerization characteristic were confirmed by kinetic studies as well as GPC and ^{1}H NMR analyses.

Experimental

Materials

MMA (99%) was washed with 5% NaOH and distilled water several times to remove the inhibitor, and freshly distilled under reduced pressure after drying over Na_2SO_4. 2,2-Azobisisobutyronitrile (AIBN) was recrystallized twice from ethanol prior to use. Dimethyl sulfoxide (DMSO, 99%), toluene (99%), and tetrahydrofuran (THF, 99%) were dried over Na_2SO_4 before use. Cupric bromide ($CuBr_2$, 99%, Aladdin), copper sulfate pentahydrate ($CuSO_4 \cdot 5H_2O$, 99%), cupric nitrate trihydrate ($Cu(NO_3)_2 \cdot 3H_2O$, 99%), cupric acetate monohydrate ($Cu(CH_3COO)_2 \cdot H_2O$, 99%), 1-methylimidazole (MIM, 99%, Aladdin), and triphenyl phosphate (Ph_3PO_4, 99%) were used as received without further purification.

Synthesis of [Phmim][Ph_2PO_4]

Triphenyl phosphate (32.63 g, 0.1 mol) and 1-methylimidazole (8.24 g, 0.1 mol) was added into a flask in sequence. Then the mixture was charged with nitrogen before sealed, and placed in an oil bath at 150 °C for 10 h. Finally, the obtained mixture was washed with petroleum ether three times to remove the unreacted triphenyl phosphate. The synthetic route of [Phmim][Ph_2PO_4] is shown in Scheme 1. Yield: 39.78 g (90 wt%). Element analysis: C 64.70%, H 5.18%, O 15.67% (calculated); C 58.76%, H 5.58%, O 14.02% (found). In addition, the ^{1}H NMR spectra of [Phmim][Ph_2PO_4] is presented in Fig. 1. The signal at 3.56–3.95 ppm is attributed to the protons of methylene group (CH_2, peak a) in imidazole, and the signals at 6.72–7.65 ppm are attributed to the protons of benzene (CH, peaks b–f).

Polymerization

A typical polymerization procedure is as follows. MMA, $CuBr_2$, AIBN, [Phmim][Ph_2PO_4], and THF with a predetermined molar ratio were added into a dry Schlenk tube. Then the tube was immersed in liquid nitrogen for one minute. Subsequently, the mixture was subject to three freeze–pump–thaw cycles to remove oxygen, charged with nitrogen, and sealed. The tube with the reaction mixture was placed in an oil bath at the predetermined reaction temperature. After a desired polymerization time, the polymerization mixture was cooled by ice water, exposed to air, and the content was then diluted with THF to achieve a homogenous solution. The polymer was then precipitated into a large excess of distilled water. The final polymer was separated by filtration, and dried under vacuum at 60 °C until a constant weight. The monomer conversion was determined gravimetrically.

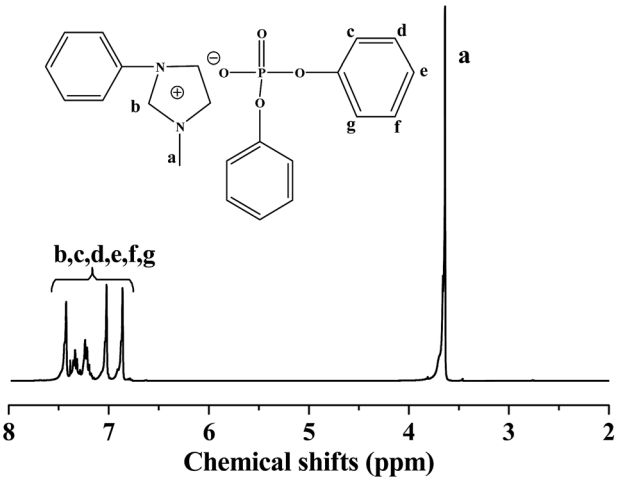

Fig. 1 ^{1}H NMR spectrum of [Phmim][Ph_2PO_4]. Reaction conditions: $[MIM]_0/[Ph_3PO_4]_0 = 1:1$, reaction time = 10 h, T = 150 °C.

Characterization

^{1}H NMR spectra of PMMA samples were recorded on a Bruker 300 MHz nuclear magnetic resonance (NMR) instrument using $CDCl_3$ as the solvent and tetramethylsilane (TMS) as the internal standard at ambient temperature. The number-average molecular weight ($M_{n,GPC}$) and PDI values of poly(methyl methacrylate) (PMMA) samples were determined by gel permeation chromatography (GPC). The GPC system contains a Waters 510 HPLC pump and Waters 2414 RI detector using three Waters Ultrastyragel columns (500, 10^3, and 10^5) in THF at a flow rate of 1.0 mL min^{-1}. The columns were calibrated by PMMA narrow standards. Elemental analysis was performed on an elemental Vario EL cube spectrophotometer with an 80 bit autosampler and a "purge-trap" adsorption analytical column.

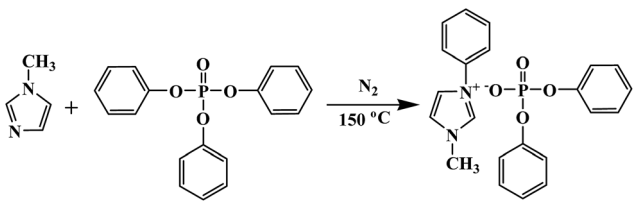

Scheme 1 Synthetic route of [Phmim][Ph_2PO_4].

Results and discussion

Copper-catalyzed reverse ATRP of MMA utilizing 1-phenyl-3-methylimidazole diphenyl phosphate ([Phmim][Ph_2PO_4]) as the ligand

As mentioned previously, ILs are not efficient ligands for copper(II)-catalyzed reverse ATRP of MMA. Therefore, we first reasoned the feasibility of IL as phosphorus-based ligands ligand for Cu(II)-catalyzed reverse ATRP. Two phosphate-anionic IL ([Bmim][DBP] and [Phmim][Ph_2PO_4]) and a common halogen

IL ([Bmim][Br]) were examined, and the results are presented in Table 1.

Obviously, with a common and simple IL 1-butyl-3-methylimidazole bromine ([Bmim][Br]), the polymerization only gives 50% monomer conversion within 25 h (entry 1). Besides, the measured molecular weight value ($M_{n,GPC}$ = 20 500) of the resultant PMMA is much larger than the theoretical one ($M_{n,th}$ = 5300), and the PDI value is as high as 1.79. These results indicate that the polymerizations have not any differences in molecular dimensions compared with the conventional radical polymerization except that it is retarded by $CuBr_2$.[34] Instead, with phosphate-anionic IL, *i.e.*, [Bmim][DBP] and [Phmim][Ph_2PO_4], the rate of polymerization enhanced greatly (entries 2 and 3). At the same time, the difference between measured molecular weight values and theoretical ones decreased considerably. The decreasing rule is also reflected in the PDI results. Particularly, [Phmim][Ph_2PO_4] provided the fastest rate of polymerization (95 monomer conversions after 25 h) and the highest control of the radical polymerization of MMA with the measured $M_{n,GPC}$ very close to theoretical $M_{n,th}$ and low PDI of 1.27 (entry 3). This may be ascribed to the fact that there exists much stronger complexation of [Phmim][Ph_2PO_4] with Cu(II) compound compared with [Bmim][Br], followed by [Bmim][DBP], and thus the increased solubility of catalytic system will avail the function of reverse ATRP process. As a result, [Phmim][Ph_2PO_4] is the optimal ligand for reverse ATRP under investigated conditions.

The polymerization catalyzed with $CuBr_2$/[Phmim][Ph_2PO_4] in presence of AIBN as the radical source was investigated in detail to follow the evolutions of molecular weight and PDI values. The $CuBr_2$–[Phmim][Ph_2PO_4] catalyzed reverse ATRP of MMA was first performed with $[MMA]_0/[AIBN]_0/[CuBr_2]_0/[IL]_0$ = 200 : 1 : 2 : 4 in THF at 70 °C. The monomer conversion and $\ln([M]_0/[M])$ *versus* reaction time are plotted in Fig. 2. Clearly, a quasi-linear semilogarithmic kinetics is observed, suggesting that the propagating radical concentrations remained almost unchanged during the polymerization process. Additionally, there is a certain deviation from linearity, suggesting the presence of unavoidable termination or transfer reactions for radical polymerization. It is also noted that there is an induction period of 8.5 h at the beginning of polymerization.[35] This indicates that the polymerization needs some time to decompose AIBN and establish a dynamic equilibrium between the Cu(I) and Cu(II) species.[36,37] Besides, the inhibition caused by a high concentration of high valence copper at the initial stage or the incomplete degassing of oxygen may also lead to a lengthened induction period.

Table 1 Effect of ILs on reverse ATRP of MMA[a]

Entry	ILs	Conv. (%)	$M_{n,th}$ (Da)	$M_{n,GPC}$ (Da)	PDI
1	[Bmim]Br	50	5300	20 500	1.79
2	[Bmim][DBP]	85	9100	16 100	1.39
3	[Phmim][Ph_2PO_4]	95	10 100	15 800	1.27

[a] $[MMA]_0/[AIBN]_0/[CuBr_2]_0/[IL]_0$ = 200 : 1 : 2 : 4, $[MMA]_0$ = 9.4 mol L^{-1}, time = 25 h, MMA/THF = 1 : 1 (v/v), T = 70 °C.

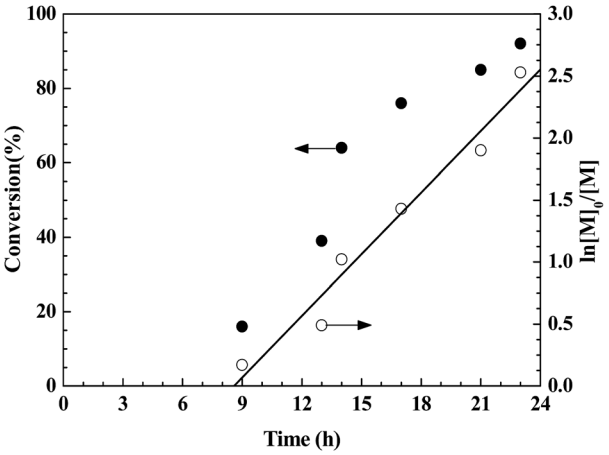

Fig. 2 Kinetic plots of $\ln([M]_0/[M])$ *versus* reaction time for reverse ATRP of MMA in THF. Reaction conditions: $[MMA]_0/[AIBN]_0/[CuBr_2]_0/[Phmim][Ph_2PO_4]_0$ = 200 : 1 : 2 : 4, $[MMA]_0$ = 9.4 mol L^{-1}, MMA/THF = 1 : 1 (v/v), T = 70 °C.

The $M_{n,th}$ of PMMA obtained from reverse ATRP can be calculated based on the following equation:[38]

$$M_{n,th} = \frac{[MMA]_0 \times Conv. \times M_{MMA}}{2[AIBN]_0(1 - e^{-k_d t})}$$

where $[MMA]_0$ and $[AIBN]_0$ correspond to the initial concentrations of MMA and AIBN, respectively. Conv. is the monomer conversion. M_{MMA} is the molecular weight of MMA. The value of k_d refers to decomposition rate at 70 °C, and t corresponds to the reaction time. Fig. 3 illustrates that the molecular weight ($M_{n,GPC}$) values of the polymers increased linearly with monomer conversions. Meanwhile, the PDI values (1.25–1.46) of the obtained PMMA samples remained low throughout the polymerization process. However, a certain deviation from linearity is observed, implying that there were unavoidable termination or transfer reactions. The result can be clearly seen in the corresponding GPC curve of the polymers (Fig. 4). The curves are

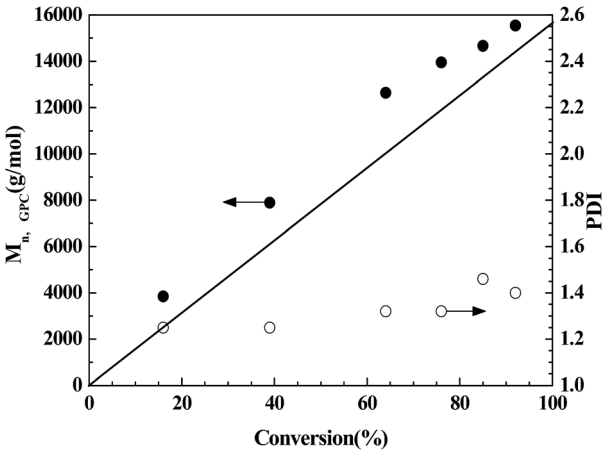

Fig. 3 Evolution of M_n (— theoretical) and PDI with monomer conversion for reverse ATRP of MMA in THF. Reaction conditions: $[MMA]_0/[AIBN]_0/[CuBr_2]_0/[Phmim][Ph_2PO_4]_0$ = 200 : 1 : 2 : 4, $[MMA]_0$ = 9.4 mol L^{-1}, MMA/THF = 1 : 1 (v/v), T = 70 °C.

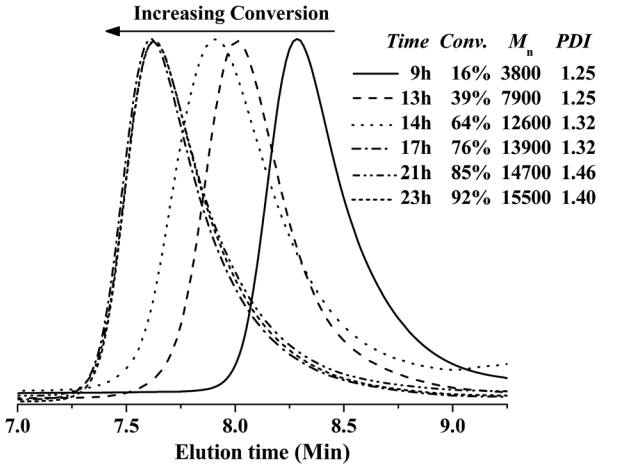

Fig. 4 Evolution of GPC traces for reverse ATRP of MMA in THF at different monomer conversions: 16%, 39%, 64%, 76%, 85%, and 92%. Reaction conditions: $[MMA]_0/[AIBN]_0/[CuBr_2]_0/[Phmim][Ph_2PO_4]_0$ = 200 : 1 : 2 : 4, $[MMA]_0 = 9.4$ mol L^{-1}, MMA/THF = 1 : 1 (v/v), $T = 70$ °C.

nearly narrow and symmetrical. Moreover, the traces of the obtained typical polymers shift toward shorter elution time, indicating the increase of $M_{n,GPC}$ with monomer conversion. Nevertheless, the GPC traces are not symmetrical at higher yields, and the molecular weight distribution curves and PDI values do not gradually decrease, indicating a partial loss of control over the polymerization. Therefore the results suggest that the $CuBr_2$–[Phmim][Ph_2PO_4]-catalyzed reverse ATRP of MMA possess the controlled/"living" radical polymerization characteristics of ATRP.[37]

Effect of solvent

The effect of various solvent on $CuBr_2$–[Phmim][Ph_2PO_4] catalyzed reverse ATRP of MMA was studied. As shown in Table 2, for the polymerization conducted in bulk, the monomer conversion reached 95% within 16 h (entry 1). The measured molecular weight value ($M_{n,GPC}$ = 13 000) is very close to the theoretical one ($M_{n,th}$ = 11 400). However, the measured PDI value is as high as 1.42. For the polymerization conducted in THF, the polymerization yielding 95% monomer conversion after 25 h (entry 2). The measured $M_{n,GPC}$ = 15 800 is slightly higher than the theoretical $M_{n,th}$ = 10 100. Particularly, the measured PDI value (PDI = 1.27) is the lowest among the investigated reaction medias. For the polymerization conducted in toluene, the polymerization achieved 96% monomer conversion within the same time (entry 3). Meanwhile, the measured molecular weight value $M_{n,GPC}$ = 13 000 match with theoretical one $M_{n,th}$ = 10 200. However, the measured PDI value is slightly high (*i.e.*, 1.42). For the polymerization conducted in DMSO, the monomer conversion only reach 26% within 25 h, and both the measured $M_{n,GPC}$ = 2600 was low (entry 4), but the measured PDI value (PDI = 1.40) is relatively high. To sum up, though bulk and toluene systems can yield fast rates of polymerizations (95% and 96% monomer conversions) and the measured PDI values reached up to 1.42. The obvious difference of the polymerization results may be attributed to the disproportionation reaction of the generated activator Cu^+ for DMSO.[39] For toluene, a nonpolar nature did not exhibit excellent solubility for the catalyst system. Therefore, THF is the optimal solvent for the investigated systems, as evidenced from the results that the corresponding polymerization obtained 95% monomer conversion, and produced well-defined PMMA with controlled $M_{n,GPC}$ (15 800) close to $M_{n,th}$ (10 100) as well as the lowest PDI value (1.27).

Table 2 Effect of solvent on reverse ATRP of MMA[a]

Entry	Solvent	Conv. (%)	$M_{n,th}$ (Da)	$M_{n,GPC}$ (Da)	PDI
1[b]	Bulk	95	11 400	13 000	1.42
2	THF	95	10 100	15 800	1.27
3	Toluene	96	10 200	13 000	1.42
4	DMSO	26	2800	2600	1.40

[a] $[MMA]_0/[AIBN]_0/[CuBr_2]_0/[Phmim][Ph_2PO_4]_0$ = 200 : 1 : 2 : 4, $[MMA]_0$ = 9.4 mol L^{-1}, time = 25 h, MMA/solvent = 1 : 1 (v/v), T = 70 °C. [b] Reaction time = 16 h.

Effect of $[AIBN]_0/[CuBr_2]_0/[IL]_0$

For an ideal reverse ATRP, it is necessary to use an appropriate molar ratio of catalyst/ligand to obtain a high control of the polymerization.[40] For the sake of comparison, the control experiment, the conventional free radical polymerization of MMA in absence of the $CuBr_2$ or IL was first carried out at 70 °C. The polymerization results are summarized in entries 1–3 of Table 3. For the conventional radical polymerization in absence of $CuBr_2$ and IL, the monomer conversion reached 91% within 10 h (entry 1). The measured molecular weight value $M_{n,GPC}$ = 35 300 is much larger than theoretical one $M_{n,th}$ = 13 500, and the PDI value is as high as 1.56. Likewise, for the polymerization system free of $CuBr_2$, the monomer conversion reached 88% within 10 h, and the measured $M_{n,GPC}$ = 33 400 is much larger than theoretical $M_{n,th}$ = 13 100, and the PDI value is 1.87 (entry 2). Finally, the polymerization with only $CuBr_2$ is greatly retarded of inhibited, yielding a low monomer conversion of 35% within 31 h as well as a low polymer molecular weight of 5600 and a high PDI value of 1.72 (entry 3). Therefore, the blank conventional radical polymerizations in presence of $CuBr_2$ or IL cannot proceed *via* reverse ATRP process and were out of control under the investigated reaction conditions.

Alternatively, effect of $[CuBr_2]_0/[IL]_0$ on the polymerization was investigated under similar reaction conditions. For entries 4–6, and 9, the molar ratio of $[CuBr_2]_0/[IL]_0$ is 1 : 2. The polymerization reached 88% and 91% monomer conversion within 25 h for $[AIBN]_0/[CuBr_2]_0/[IL]_0$ = 1 : 0.5 : 1 and 1 : 1 : 2, respectively (entries 4–5). For $[AIBN]_0/[CuBr_2]_0/[IL]_0$ = 1 : 2 : 4, the polymerization gived 95% monomer conversion within 25 h (entry 6). Decreasing $[AIBN]_0/[CuBr_2]_0/[IL]_0$ down to 1 : 4 : 8, the polymerization yield 98% conversion within 25 h (entry 9). Thus lowering the molar ratio of $[AIBN]_0/[CuBr_2]_0/[IL]_0$ can slightly enhance the monomer conversion. The same rule can be seen from the evolution of the molecular weight and PDI values with different $[AIBN]_0/[CuBr_2]_0/[IL]_0$ values, as shown in Table 3,

Table 3 Effect of molar ratio of $CuBr_2$ to IL on reverse ATRP of MMA[a]

Entry	$[MMA]_0/[AIBN]_0/[CuBr_2]_0/[IL]_0$	Time (h)	Conv. (%)	$M_{n,th}$ (Da)	$M_{n,GPC}$ (Da)	PDI
1	200/1/0/0	10	91	13 500	35 300	1.56
2	200/1/0/4	10	88	13 100	33 400	1.87
3	200/1/2/0	31	35	3600	5600	1.72
4	200/1/0.5/1	25	88	9400	19 100	1.32
5	200/1/1/2	25	91	9700	16 300	1.27
6	200/1/2/4	25	95	10 100	15 800	1.27
7	200/1/2/6	25	94	10 000	21 600	1.39
8	200/1/2/8	25	92	9800	17 100	1.37
9	200/1/4/8	25	98	10 400	25 200	1.38

[a] IL: $[Phmim][Ph_2PO_4]$, $[MMA]_0 = 9.4$ mol L^{-1}, MMA/THF = 1 : 1 (v/v), $T = 70$ °C.

Fig. 5 and 6. With a high $[AIBN]_0/[CuBr_2]_0/[IL]_0$ value of 1 : 0.5 : 1, the corresponding PDI value is 1.32. With the decrease of $[AIBN]_0/[CuBr_2]_0/[IL]_0$ down to 1 : 1 : 2 and 1 : 2 : 4, the corresponding PDI values remain 1.27. Further decreasing the molar ratio of $[AIBN]_0/[CuBr_2]_0/[IL]_0$ to 1 : 4 : 8, the corresponding PDI value increased up to 1.38. In case of molecular weight, with the $[AIBN]_0/[CuBr_2]_0/[IL]_0$ of 1 : 2 : 4, the measured $M_{n,GPC}$ = 15 800 is the closest to theoretical $M_{n,th}$ = 10 100 among the four catalytic systems *i.e.* the initiator efficiency is the highest (Fig. 6). For entries 6–8, the monomer conversion decrease with increase of the amount of IL ($[CuBr_2]_0/[IL]_0$ = 2 : 4, 2 : 6, and 2 : 8). With a molar ratio of $[CuBr_2]_0/[IL]_0 = 2 : 4$, the measured $M_{n,GPC}$ is close to theoretical one, and the PDI value (1.27) is the lowest among three polymerizations. Therefore, all these results indicate that selecting a suitable molar ratio of $[CuBr_2]_0/[IL]_0 = 2 : 4$ is extremely important for reverse ATRP of MMA.

Effect of reaction temperature

Reaction temperature was also investigated in order to reduce polymerization duration and improve the control of molecular weight and PDI. For the temperature of 60–80 °C, the polymerizations yielded higher monomer conversions than 90 °C after 25 h (entries 1–3 in Table 4). However, when the temperature increased up to 90 °C, a lower monomer conversion of 75% within 25 h is observed (entry 4). The decrease in rate of polymerization is attributed to the high primary radical concentration at the start of the polymerization and the accompanying relatively fast rate of biradical termination, leading to the insufficient supply of reactive radicals at the later stage of polymerization.[41] Concerning the control over the molecular weights at four investigated temperature, the polymers of higher molecular weight higher than 14 000 were all obtained, and the difference between measured molecular weight value and theoretical one tended to enlarge with the increase of reaction temperature. Nevertheless, more attention should be paid to the influence of reaction temperature on the PDI. Clearly, a lower temperature of 60 °C or higher temperatures of 80 and 90 °C will increase the PDI results. Comparatively speaking, 70 °C is an optimal temperature to provide a low PDI value of 1.27 together with a higher monomer conversion and controlled molecular weight of polymer.

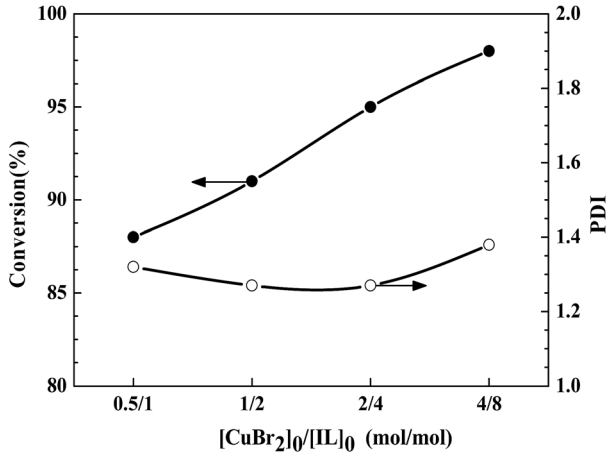

Fig. 5 Dependence of conversion and PDI on the molar ratio of $[CuBr_2]_0/[Phmim][Ph_2PO_4]_0$ for reverse ATRP of MMA in THF. Reaction conditions: $[MMA]_0/[AIBN]_0 = 200 : 1$, MMA/THF = 1 : 1 (v/v), $[MMA]_0$ = 9.4 mol L^{-1}, $T = 70$ °C.

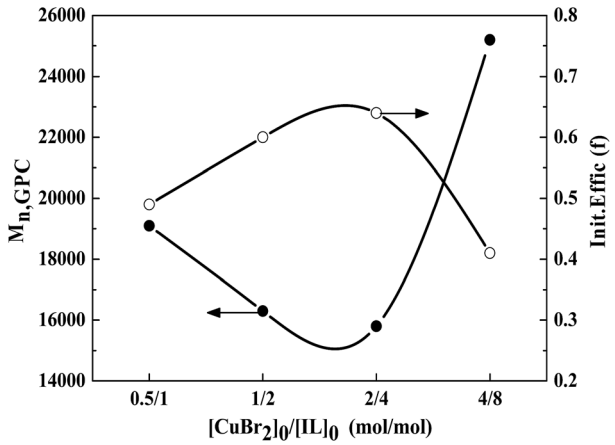

Fig. 6 Dependence of $M_{n,GPC}$ and initiator efficiency (f) on the molar ratio of $[CuBr_2]_0/[Phmim][Ph_2PO_4]_0$ for reverse ATRP of MMA in THF. Reaction conditions: $[MMA]_0/[AIBN]_0 = 200 : 1$, MMA/THF = 1 : 1 (v/v), $[MMA]_0$ = 9.4 mol L^{-1}, $T = 70$ °C.

Table 4 Effect of temperature on reverse ATRP of MMA[a]

Entry	Temperature (°C)	Conv. (%)	$M_{n,th}$ (Da)	$M_{n,GPC}$ (Da)	PDI
1	60	94	9400	14 300	1.38
2	70	95	10 100	15 800	1.27
3	80	95	9500	26 900	1.32
4	90	75	7500	10 700	1.31

[a] $[MMA]_0/[AIBN]_0/[CuBr_2]_0/[Phmim][Ph_2PO_4]_0 = 200:1:2:4$, $[MMA]_0 = 9.4$ mol L^{-1}, time = 25 h, MMA/THF = 1 : 1 (v/v).

Chain-end functionality

The structure of PMMA obtained at 16% monomer conversion ($M_{n,GPC} = 3800$, PDI = 1.25) *via* $CuBr_2$–[Phmim][Ph_2PO_4] catalyzed reverse ATRP with $[MMA]_0/[AIBN]_0/[CuBr_2]_0/[Phmim][Ph_2PO_4]_0 = 200:1:2:4$ is characterized by ^{1}H NMR technique. As exhibited in Fig. 7, the chemical shift at 0.65–1.25 ppm was reasonably assigned to the protons of methyl protons (CH_3, peak b). The chemical shift at 1.33–2.10 ppm was attributed to methylene protons (CH_2, peak a) in the main chain. The chemical shift at 3.48–3.71 ppm was attributed to methoxy protons (OCH_3, peak c). Moreover, the chemical shift at 3.74–3.84 ppm corresponded to the protons of OCH_3 adjacent to the bromine atom (peak d), proving the presence of the containing-halogen end group, $CH_2CCl(CH_3)(COOCH_3)$, which is consistent with the literature reports.[42] The $M_{n,NMR}$ (3100) value can be calculated from the ratio of the methylene protons (peak a) to the terminal ones (peak d), which is very close to the $M_{n,GPC}$ (3800), indicating that the PMMA is end-capped by Br with high fidelity. Thus the radical polymerization of MMA mediated by $CuBr_2$–[Phmim][Ph_2PO_4] follows the reverse ATRP mechanism.

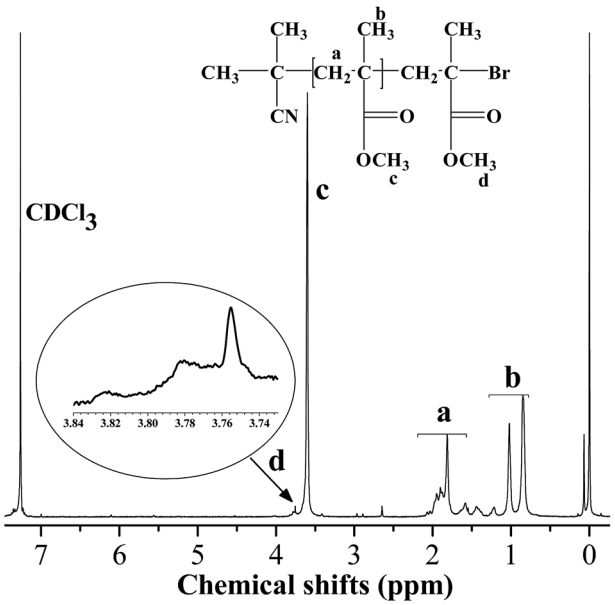

Fig. 7 ^{1}H NMR spectrum of PMMA obtained from reverse ATRP of MMA in THF. Reaction conditions: $[MMA]_0/[AIBN]_0/[CuBr_2]_0/[Phmim][Ph_2PO_4]_0 = 200:1:2:4$, $[MMA]_0 = 9.4$ mol L^{-1}, MMA/THF = 1 : 1 (v/v), reaction time = 9 h, monomer conversion = 16%, $T = 70$ °C.

Conclusions

Facile, simple, and inexpensive ionic liquid (IL), 1-phenyl-3-methylimidazole diphenyl phosphate ([Phmim][Ph_2PO_4]), has been successfully used as efficient phosphorus ligand for $CuBr_2$-mediated reverse ATRP. The results show that IL provided the optimal controlled/living nature, as evidenced from ideal rate of polymerization, well control of molecular weight and PDI values, and bromine-containing chain-end fidelity confirmed by ^{1}H NMR spectroscopy. Varied experimental parameters including solvent, reaction temperature, IL, and molar ratio of $CuBr_2$/[Phmim][Ph_2PO_4] were tested to improve the control of the polymerization. Thus we believe that the facile, inexpensive, and simple catalytic system, the combination of phosphate IL and high-valence copper compound, provides a simple and efficient approach to reverse ATRP reactions of various vinyl monomers.

Conflicts of interest

There are no conflicts to declare.

Acknowledgements

The authors are grateful for subsidy provided by the National Natural Science Foundation of China (No. 21074127).

Notes and references

1 P. Krys, H. Schroeder, J. Buback, M. Buback and K. Matyjaszewski, *Macromolecules*, 2016, **49**, 7793–7803.
2 P. Leophairatana, S. Samanta, C. C. De Silva and J. T. Koberstein, *J. Am. Chem. Soc.*, 2017, **139**, 3756–3766.
3 T. G. Ribelli, S. Wahidur Rahaman, J. C. Daran, P. Krys, K. Matyjaszewski and R. Poli, *Macromolecules*, 2016, **49**, 7749–7757.
4 G. Wang, M. Schmitt, Z. Wang, B. Lee, X. Pan, L. Fu, J. Yan, S. Li, G. Xie and M. R. Bockstaller, *Macromolecules*, 2016, **49**, 8605–8615.
5 Q. Yang, J. Lalevée and J. Poly, *Macromolecules*, 2016, **49**, 7653–7666.
6 K. Matyjaszewski, *Macromolecules*, 2012, **45**, 4015–4039.
7 J. C. Theriot, C. H. Lim, H. Yang, M. D. Ryan, C. B. Musgrave and G. M. Miyake, *Science*, 2016, **352**, 1082–1086.
8 J. Ran, L. Wu, Z. Zhang and T. Xu, *Prog. Polym. Sci.*, 2014, **39**, 124–144.
9 X. H. Liu, F. J. Zhang, H. N. Li, X. H. Hu, W. L. Di and S. Zhao, *J. Appl. Polym. Sci.*, 2015, **132**, 2410–2415.
10 J. S. Wang and K. Matyjaszewski, *J. Am. Chem. Soc.*, 1995, **117**, 5614–5615.
11 J. Xia and K. Matyjaszewski, *Macromolecules*, 1997, **30**, 7692–7696.
12 A. Anastasaki, C. Waldron, P. Wilson, R. McHale and D. M. Haddleton, *Polym. Chem.*, 2013, **4**, 2672–2675.
13 Y. H. Yu, X. H. Liu, D. Jia, B. W. Cheng, F. J. Zhang, H. N. Li, P. Chen and S. Xie, *J. Polym. Sci., Part A: Polym. Chem.*, 2013, **51**, 1468–1474.

14 X. H. Liu, J. Wang, J. S. Yang, S. L. An, Y. L. Ren, Y. H. Yu and P. Chen, *J. Polym. Sci., Part A: Polym. Chem.*, 2012, **50**, 1933–1940.
15 W. Tang and K. Matyjaszewski, *Macromol. Theory Simul.*, 2008, **17**, 359–375.
16 C. Boyer, A. H. Soeriyadi, P. B. Zetterlund and M. R. Whittaker, *Macromolecules*, 2016, **44**, 8028–8033.
17 A. Anastasaki, V. Nikolaou, G. Nurumbetov, N. P. Truong, G. S. Pappas, N. G. Engelis, J. F. Quinn, M. R. Whittaker, T. P. Davis and D. M. Haddleton, *Macromolecules*, 2015, **48**, 5140–5147.
18 Y. Zhou, L. Qiu, Z. Deng, J. Texter and F. Yan, *Macromolecules*, 2011, **44**, 7948–7955.
19 S. G. N. Brusseau, O. Boyron, C. Schikaneder, C. C. Santini and B. Charleux, *Macromolecules*, 2010, **44**, 215–220.
20 C. Hou, R. Qu, C. Ji, C. Sun and C. Wang, *J. Polym. Sci., Part A: Polym. Chem.*, 2008, **46**, 2701–2707.
21 Y. Liang, H. Chen and W. Zhou, *J. Macromol. Sci., Part A: Pure Appl.Chem.*, 2009, **46**, 759–764.
22 H. Chen, Y. Meng, Y. Liang, Z. Lu and P. Lv, *J. Mater. Res.*, 2009, **24**, 1880–1885.
23 J. Ma, H. Chen, M. Zhang and M. Yu, *J. Polym. Sci., Part A: Polym. Chem.*, 2015, **50**, 609–613.
24 G. Wang, M. Lu, M. Zhong and H. Wu, *J. Polym. Res.*, 2012, **19**, 1–6.
25 X. Du, J. Pan, M. Chen, L. Zhang, Z. Cheng and X. Zhu, *Chem. Commun.*, 2014, **50**, 9266–9269.
26 Z. Deng, L. Qiu, L. Bai, Y. Zhou, B. Lin, J. Zhao, Z. Cheng, X. Zhu and F. Yan, *J. Polym. Sci., Part A: Polym. Chem.*, 2012, **50**, 1605–1610.
27 A. J. Carmichael, D. M. Haddleton, S. A. Bon and K. R. Seddon, *Chem. Commun.*, 2000, 1237–1238.
28 T. Sarbu and K. Matyjaszewski, *Macromol. Chem. Phys.*, 2001, **202**, 3379–3391.
29 G. Q. Lai, F. M. Ma, Z. Q. Hu, H. Y. Qiu, J. X. Jiang, J. R. Wu, L. M. Chen and L. B. Wu, *Chin. Chem. Lett.*, 2007, **18**, 601–604.
30 F. Ma, W. Li, G. Lai, J. Guo, M. Ruan and W. Qin, *J. Test. Eval.*, 2011, **39**, 967–973.
31 H. Ma, X. Wan, X. Chen and Q. F. Zhou, *J. Polym. Sci., Part A: Polym. Chem.*, 2003, **41**, 143–151.
32 H. Ma, X. Wan, X. Chen and Q. F. Zhou, *Polymer*, 2003, **44**, 5311–5316.
33 H. Chen, Y. Liang, M. Wang, P. Lv and Y. Xuan, *Chem. Eng. J.*, 2009, **147**, 297–301.
34 K. Matyjaszewski, A. K. Nanda and W. Tang, *Macromolecules*, 2005, **38**, 2015–2018.
35 X. H. Liu, H. N. Li, F. J. Zhang, S. Xie, Z. J. Liu and Y. G. Li, *Chin. J. Polym. Sci.*, 2015, **33**, 362–370.
36 Y. H. Yu, X. H. Liu, D. Jia, B. W. Cheng, Y. L. Ren, F. J. Zhang, H. N. Li, P. Chen and S. Xie, *J. Polym. Sci., Part A: Polym. Chem.*, 2013, **51**, 1690–1694.
37 Y. H. Yu, X. H. Liu, D. Jia, B. W. Cheng, F. J. Zhang, P. Chen and S. Xie, *Polymer*, 2013, **54**, 148–154.
38 J. S. Wang and K. Matyjaszewski, *Macromolecules*, 1995, **28**, 7572–7573.
39 Y. H. Yu, X. H. Liu, D. Jia, B. W. Cheng, F. J. Zhang, P. Chen and S. Xie, *J. Polym. Sci., Part A: Polym. Chem.*, 2013, **51**, 1559–1564.
40 X. Liu, Q. Zhu, Q. Zhang, Y. Zhang and C. Ding, *RSC Adv.*, 2017, **7**, 6972–6980.
41 T. G. Ribelli, D. Konkolewicz, X. Pan and K. Matyjaszewski, *Macromolecules*, 2014, **47**, 6316–6321.
42 W. Zhang, X. Zhu, J. Zhu and Z. Cheng, *Macromol. Chem. Phys.*, 2004, **205**, 806–813.